Stanford Exploration Project, Report 72, December 18, 1997, pages 1–103

Stanford Exploration Project, Report 72, December 18, 1997, pages 1–103

Modeling a discrete system by eigenvalue decomposition

Carlos A. Cunha Filho[1]

keywords: *modeling, two-dimensional, wave equation, Fourier transform, one-dimensional, displacement*

ABSTRACT

Numerical solutions of the wave equation require the discretization of the spatial and temporal dimensions, which creates numerical artifacts such as dispersion. If the physical system is already spatially discrete, the exact solution will be truly dispersive. The intrinsically dispersive character of these systems are a result of the constraints in the energy flux between neighbor cells of the system. Using the eigenvalue decomposition of the spatial operator I solve, exactly, the equations of motion associated with 1 and 2-D transverse isotropic spatially discrete systems. The method is unconditionally stable and requires no time discretization, but the cost is prohibitively high for practical uses. The intrinsically dispersive character of these systems are a result of the constraints in the energy flux between neighbor cells of the system. To overcome the high cost of the eigenvalue decomposition method, I have implemented an approximate solution using a time recursive scheme in a parallel architecture, with results that show good agreement with the exact solution.

INTRODUCTION

Wave propagation in the Earth is usually described in terms of the space-time partial differential wave equation (acoustic or elastic), which governs the mechanical behavior of continuous media. The basic requirement for the applicability of the wave equation is that the displacements and its first order spatial derivatives be continuous; in other words, the medium must be continuous. Evidently, this assumption has proved to be a reasonably good approximation for the behavior of Earth within the wavelength range of typical reflection seismology experiments. It is possible, however, that in some cases a discrete system might better approximate the real earth than a continuous system would. Furthermore, any practical solution of the wave equation involves its discretization in both time and space, which brings some degree of inaccuracy to the solution. Although several high-order methods have been developed to overcome

[1]**email:** not available

these numerical artifacts (see Etgen 1989 for a general discussion), it is worthwhile to consider the possibility that some of these so called "artifacts" have a physical existence and should be present in a more realistic simulation of wave propagation in the earth.

A spatially discrete system can be solved exactly, without the need of any numerical approximation. In this paper I compare the exact solution of a discrete system with the exact solution of the equivalent continuous system for some very simple 1-D models. Next, I derive the equations of motion for a 2-D discrete transverse isotropic medium and describe two methods of solution; one exact, using eigenvalue decomposition, and the other an approximation which is based in a recursive time relation.

1-D discrete systems

Let's first consider a discrete 1-D elastic medium such as that represented in Figure **??**. Two characteristics distinguish this medium from the continuous 1-D medium whose behavior is described by the wave equation. First, energy is localized in discrete points in space. Second, the internal forces are dissociated from mass, which implies that traction is not continuous since each mass is considered as a rigid body.

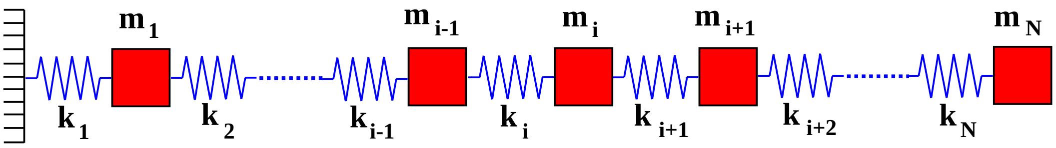

Figure 1: a spring-mass model for 1D-wave propagation in a discrete system. carlos2-springmodel [NR]

Newton's law applied to the ith mass of Figure **??** leads to the following equation:

$$m_i \frac{d^2 u_i(t)}{dt^2} = k_i u_{i-1}(t) - (k_i + k_{i+1}) u_i(t) + k_{i+1} u_{i+1}(t), \tag{1}$$

where $u_i = y_i - y_i^0$ is the displacement of mass i relative to its equilibrium position y_i^0 at time zero. The reference positions remain the same, while the equilibrium positions are a function of time.

The system of equations defined by equation (1) with $i = 1, N$ can be expressed as

$$\frac{d^2 \mathbf{u}(t)}{dt^2} = \mathbf{A}\mathbf{u}(t), \tag{2}$$

where

$$\mathbf{A} = \begin{pmatrix} \frac{-k_1-k_2}{m_1} & \frac{k_2}{m_1} & 0 & . & . & . & . & 0 \\ \frac{k_2}{m_2} & \frac{-k_2-k_3}{m_2} & \frac{k_3}{m_2} & 0 & . & . & . & 0 \\ 0 & \frac{k_3}{m_3} & \frac{-k_3-k_4}{m_3} & \frac{k_4}{m_3} & 0 & . & . & 0 \\ \vdots & \vdots & \ddots & \ddots & \ddots & \vdots & \vdots & \vdots \\ 0 & . & 0 & \frac{k_i}{m_i} & \frac{-k_i-k_{i+1}}{m_i} & \frac{k_{i+1}}{m_i} & 0 & 0 \\ \vdots & \vdots & \vdots & \vdots & \ddots & \ddots & \ddots & \vdots \\ 0 & . & . & . & 0 & \frac{k_{N-1}}{m_{N-1}} & \frac{-k_{N-1}-k_N}{m_{N-1}} & \frac{k_N}{m_{N-1}} \\ 0 & . & . & . & . & 0 & \frac{-k_N}{m_N} & \frac{k_N}{m_N} \end{pmatrix}.$$

This is a second-order system of N ordinary differential equations in time for the N unknown functions $\mathbf{u_i(t)}$. To find the solution, the pair of initial conditions $u(0)$ and $d\mathbf{u(0)}/dt$ must be specified. For the continuous case, the wave equation has also a second-order space differentiation, and thus requires two boundary conditions. Here, these two conditions correspond to the first and last equations.

Fourier transforming equation (2) over time results in

$$-\omega^2\mathbf{u}(\omega) = \mathbf{A}\mathbf{u}(\omega), \tag{3}$$

which represents an eigenvalue decomposition problem. For each eigenvalue ($\lambda_i = -\omega_i^2$) there will be two frequencies: $\omega_i^+ = +\sqrt{-\lambda}$ and $\omega_i^- = -\sqrt{-\lambda}$.

Let $\mathbf{E}$ be the matrix formed by the eigenvectors $\mathbf{e_i}$ of $\mathbf{A}$ and $\mathbf{\Lambda}$ the diagonal matrix with the respective eigenvalues. If $\mathbf{A}$ is Hermitian, then the set of eigenvectors $\mathbf{e_i}$ form a complete orthonormal basis for $\mathbf{u}$. If the masses are identical $\mathbf{A}$ is real-symmetric and the general solution $\mathbf{u}(\omega)$ is given by

$$\mathbf{u}(\omega) = \sum_{i=1}^{N} a_i\mathbf{e_i}\delta(\omega - \omega_i) + b_i\mathbf{e_i}\delta(\omega + \omega_i), \tag{4}$$

which in the time domain corresponds to

$$\mathbf{u}(t) = \sum_{i=1}^{N} \mathbf{e_i}\ \{a_i\ e^{-\omega_i t} + b_i\ e^{+\omega_i t}\}$$

or, after some manipulation,

$$\mathbf{u}(t) \quad = \quad \mathbf{E} \quad [\cos(\mathbf{\Omega}t) \quad \sin(\mathbf{\Omega}t)] \quad \begin{pmatrix} \mathbf{c} \\ \mathbf{d} \end{pmatrix}, \tag{5}$$

where $\mathbf{\Omega} = (-\mathbf{\Lambda})^{\frac{1}{2}}$. Therefore, $\cos(\mathbf{\Omega}t)$ and $\sin(\mathbf{\Omega}t)$ are N by N diagonal matrices with $\cos(\omega_i t)$ and $\sin(\omega_i t)$, respectively, in the diagonals, and $\mathbf{c}$ and $\mathbf{d}$ are constant vectors of dimension N to be determined by the initial conditions.

Applying the initial conditions to equation (5) and recalling that $\mathbf{E}$ is orthonormal, we find the equation for the unknowns $\mathbf{c}$ and $\mathbf{d}$:

$$\begin{pmatrix} \mathbf{c} \\ \mathbf{d} \end{pmatrix} = \begin{bmatrix} \mathbf{I} & \mathbf{0} \\ \mathbf{0} & \mathbf{\Omega^{-1}} \end{bmatrix} \begin{bmatrix} \mathbf{E^T} & \mathbf{0} \\ \mathbf{0} & \mathbf{E^T} \end{bmatrix} \begin{pmatrix} \mathbf{u}(0) \\ \dot{\mathbf{u}}(0) \end{pmatrix}.$$

Substituting this result in equation (5) and in the equivalent relation for $\dot{\mathbf{u}}(t)$ results in

$$\begin{pmatrix} \mathbf{u}(t) \\ \dot{\mathbf{u}}(t) \end{pmatrix} = \begin{bmatrix} \mathbf{E} & \mathbf{0} \\ \mathbf{0} & \mathbf{E} \end{bmatrix} \begin{bmatrix} \cos(\mathbf{\Omega}t) & \mathbf{\Omega}^{-1}\sin(\mathbf{\Omega}t) \\ -\mathbf{\Omega}\sin(\mathbf{\Omega}t) & \cos(\mathbf{\Omega}t) \end{bmatrix} \begin{bmatrix} \mathbf{E^T} & \mathbf{0} \\ \mathbf{0} & \mathbf{E^T} \end{bmatrix} \begin{pmatrix} \mathbf{u}(0) \\ \dot{\mathbf{u}}(0) \end{pmatrix}. \tag{6}$$

Figure **??** compares the exact, analytical solution of the wave equation (**??**-a) with the discrete-model solution (**??**-b) from equation (6). The initial conditions are $\dot{\mathbf{u}}(0) = 0$ and $\mathbf{u}(0) = (0, ..., 0, 1, 0, ..., 0)$. There are two important differences between the two cases: the dispersive character of the propagating wave-packet in the discrete case, and the continuing irradiation of energy from the impulsive source position, which is also only present in the discrete case. In both cases the spectrum is characterized by a discrete set of frequencies because the model is spatially bounded, but, while in the continuous case the set is infinite, in the discrete case only N components are present which implies an upper frequency limit.

A clear picture of the dispersion process can be obtained from the eigenvalue-eigenvector structure. Each eigenvector $\mathbf{e_i}$ corresponds to a spatial harmonic associated with the eigenfrequency ω_i. If we Fourier transform these eigenvectors and rescale the vertical axis by 2π, the resulting matrix $\tilde{\mathbf{E}}$ will represent the spatial spectra of the model. To get the dispersion relation it is necessary to stretch the horizontal axis using the eigenfrequencies ω_i, so that the spectra will be a function of ω instead of i. Figure **??** compares the $\kappa(\omega)$ spectrum obtained with this process with the dispersion relation predicted by the wave equation (continuous line) and with the function $\kappa = \omega_{max}\sin(\kappa\pi/2\kappa_{max})$ (dashed line) predicted by the discretized wave equation (Claerbout, 1985). The dispersion relation shown in this figure was generated from the eigen-spectrum of a three-layer model. *The relation between the maximum spatial and temporal frequencies $\omega_{max} = 2v\kappa_{max}/\pi$ is valid not only for the discrete case but also for the continuous case.* The meaning of such relation is that the minimum time interval for transmission of energy between adjacent points is equal to half the fundamental period $\sqrt{k/m}$. The difference is that $\kappa_{max} = \infty$ for the continuous case while $\kappa_{max} = \pi/\delta l$ for a discrete system with distance δl between masses.

The intrinsically dispersive character of wave propagation in a discrete medium can also be related to the entropic behavior of a discrete system. In a continuous medium, the constraints imposed by the continuity of stresses and displacements represent a hampering of the process of the increasing of entropy, while in a discrete system, the extra degree of freedom (no continuity constraints) allows the system to evolve into less ordered states of movement.

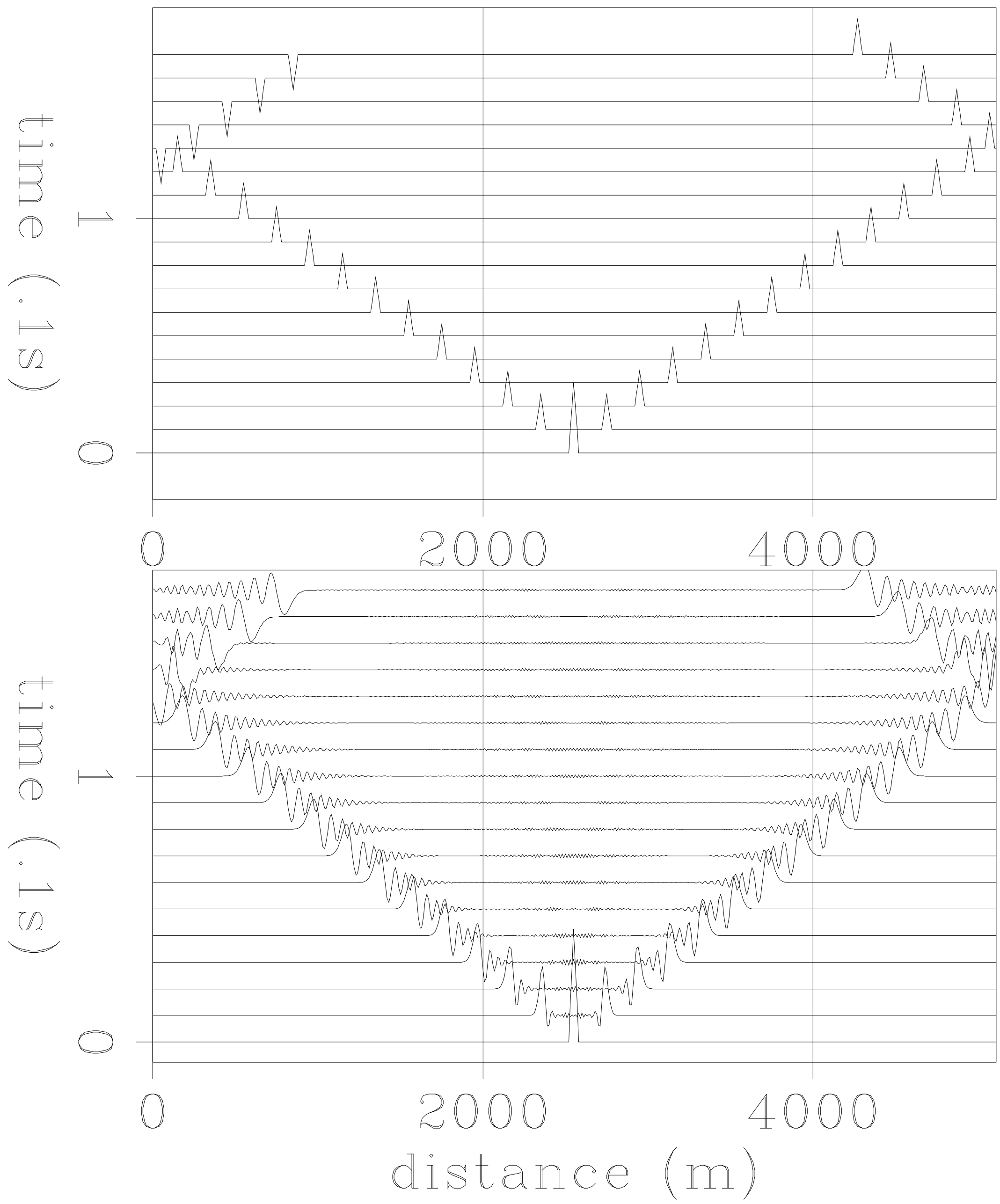

Figure 2: A comparison of *(a)* a continuous medium solution and *(b)* a discrete medium solution for the 1-D case. carlos2-s1d1 [ER]

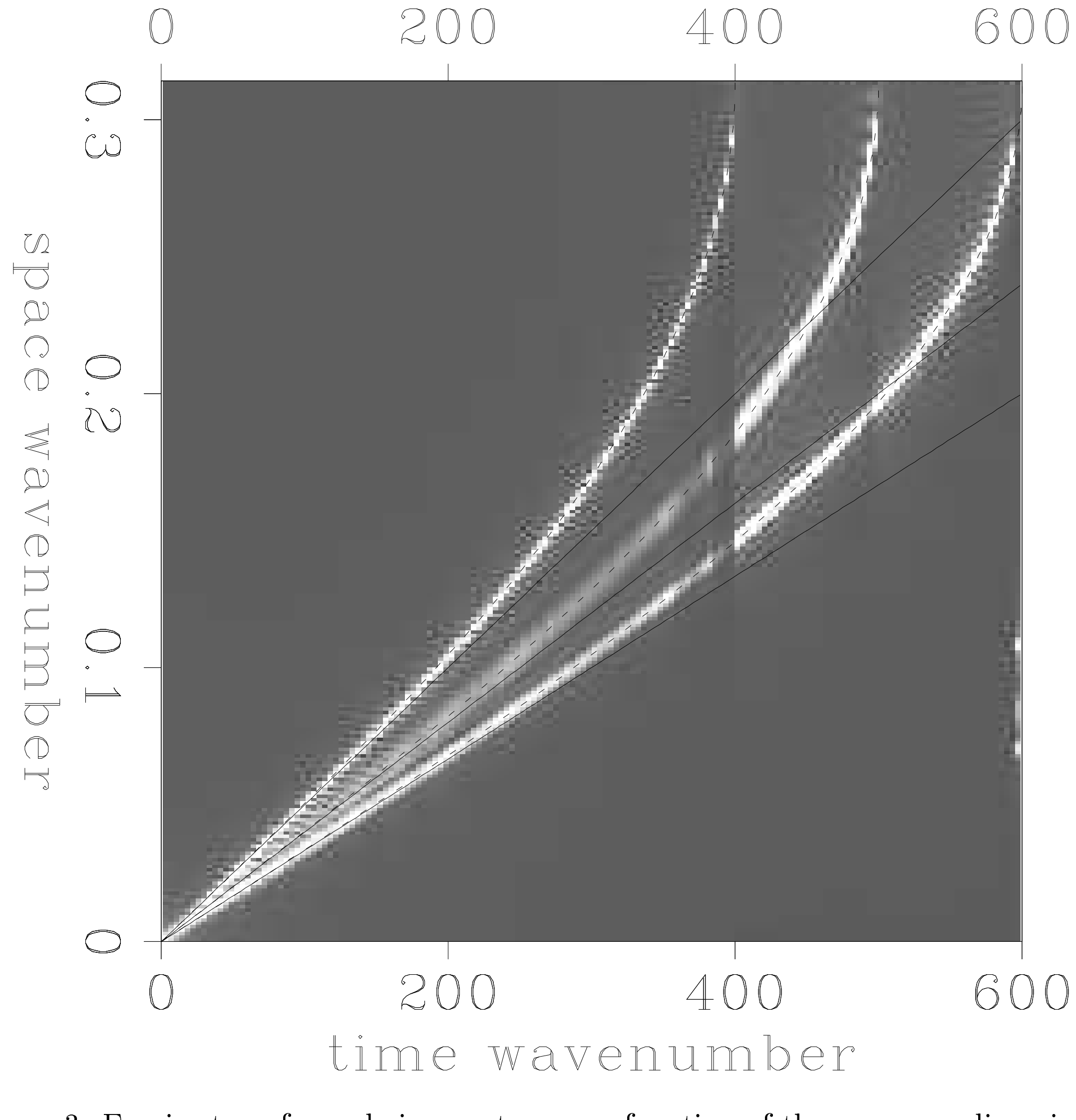

Figure 3: Fourier transformed eigenvectors as a function of the corresponding eigenfrequencies. The straight lines correspond to the constant velocities of each layer, as predicted by wave theory, while the dashed lines are $\omega_{max} \sin(\kappa\pi/2\kappa_{Nyquist})$. carlos2-kofw [ER]

2-D transverse-isotropic media

The discrete representation for the 2-D case, as well as the derivation of dynamic equations, are presented in Appendix A.

In the 2-D case equation (3) keeps the same form but $\mathbf{u}$ is now a one-dimensional representation of the bi-dimensional displacement field. If we use indices i and j to specify a given cell (or a position in the plane), and indices x and z to denote the horizontal and vertical components of $\mathbf{u}$, the one-dimensional representation of $\mathbf{u}$ will be a $2 \times N \times M$ vector given by

$$\mathbf{u} = (u_x^{1,1}, u_x^{2,1}, \ldots, u_x^{N,1}, u_x^{1,2}, u^{2,2}, \ldots, u_x^{N,M}, u_z^{1,1}, u_z^{2,1}, \ldots, u_z^{N,M}),$$

where N and M are, respectively, the horizontal and vertical dimensions of the model, as measured in terms of the number of cells.

Appendix A shows that for a 2-D system, the operator $\mathbf{A}$ of equation (3) takes the form of a $2NM \times 2NM$ sparse matrix with diagonal structure. This operator has only 13 effective terms corresponding to 17 non-vanishing diagonals as illustrated in Figure **??**, which was computed for an isotropic model of size 8 by 8 (64 cells).

Figure **??** shows the "equivalent differencing stars" associated with $\mathbf{A}$ for the case of a homogeneous medium. It's worthwhile to notice that the $u_x - u_x$ star for C_{55} represents an x-smoothed version of $\partial^2/\partial z^2$. This form is similar to the McClellan transform used by Hale (1990) to construct a numerically isotropic 3-D migration operator. Here however, the suitable form of the star comes naturally, from the direct application of physical laws.

The method is implemented here by first reducing the operator to tridiagonal form using an algorithm based in Givens rotations and then using a tridiagonal eigenvalue decomposition routine. For an n by n matrix, the cost in both stages (reduction and decomposition) is proportional to n^3, which in this case represents $8(N \times M)^3$. Whereas the cost in the reduction stage can be substantially reduced with the use of a more specific algorithm that takes advantage of the sparseness of $\mathbf{A}$, the price of the decomposition stage is still extremely high.

Figure **??** shows a time frame of the horizontal component of the displacement wavefield evaluated with the eigenvalue-decomposition modeling for a two-layer model. The upper part ($\sim 3/4$) is isotropic, while the bottom is transverse isotropic, with a total size of 37 by 37 cells, and a vertical impulsive displacement source at the center.

Recursive solution in the time domain

Although the eigenvalue decomposition is unconditionally stable and precise, the N^3-dependence of the computation time makes it prohibitively expensive. To make the method affordable, I have derived a scheme that uses a time propagator operator to find the solution at time $t + \Delta t$, using only the solution at time t. The basic principle

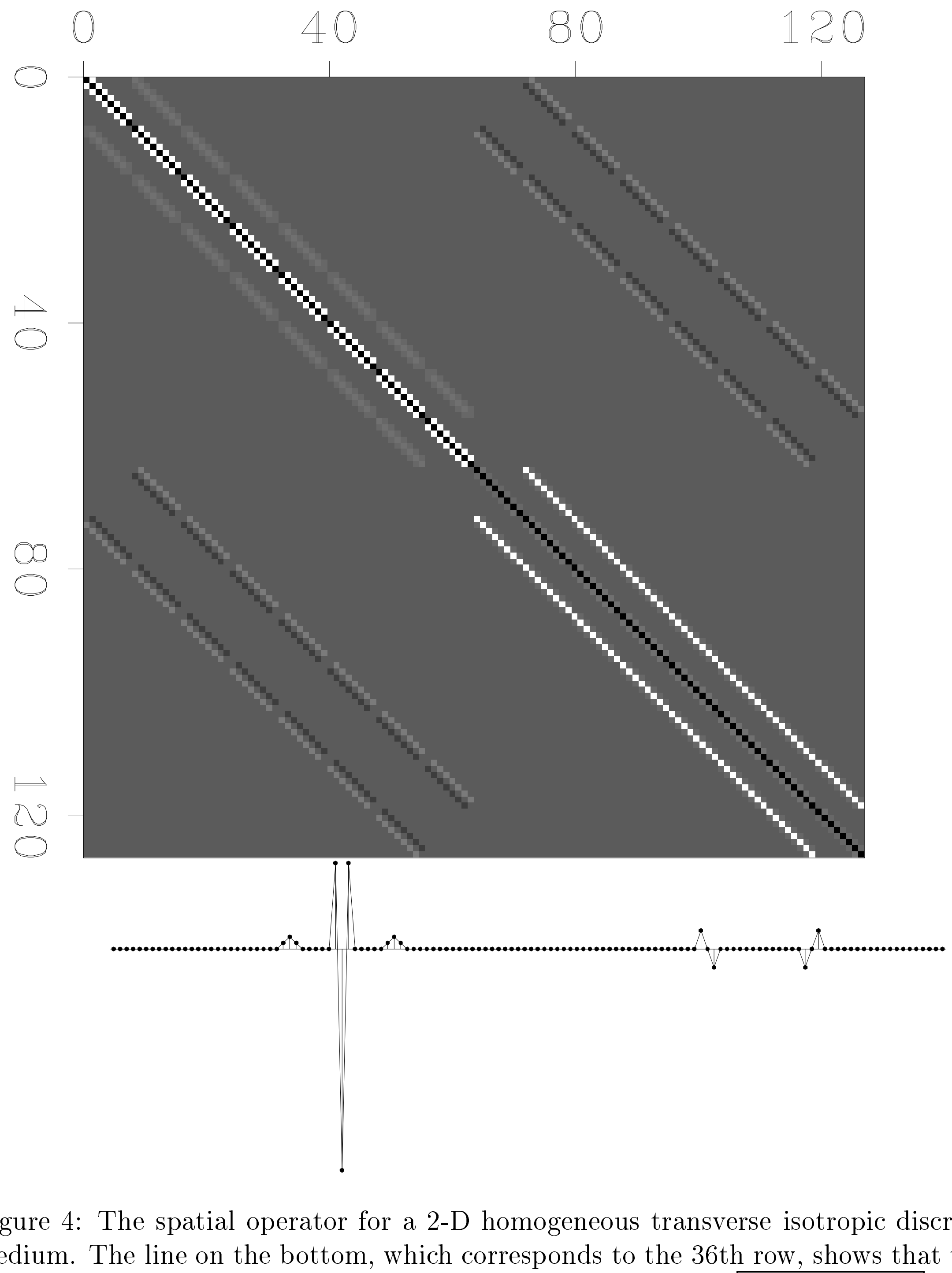

Figure 4: The spatial operator for a 2-D homogeneous transverse isotropic discrete medium. The line on the bottom, which corresponds to the 36th row, shows that the operator has 13 effective terms, or 17 non-vanishing diagonals. carlos2-2doper [ER]

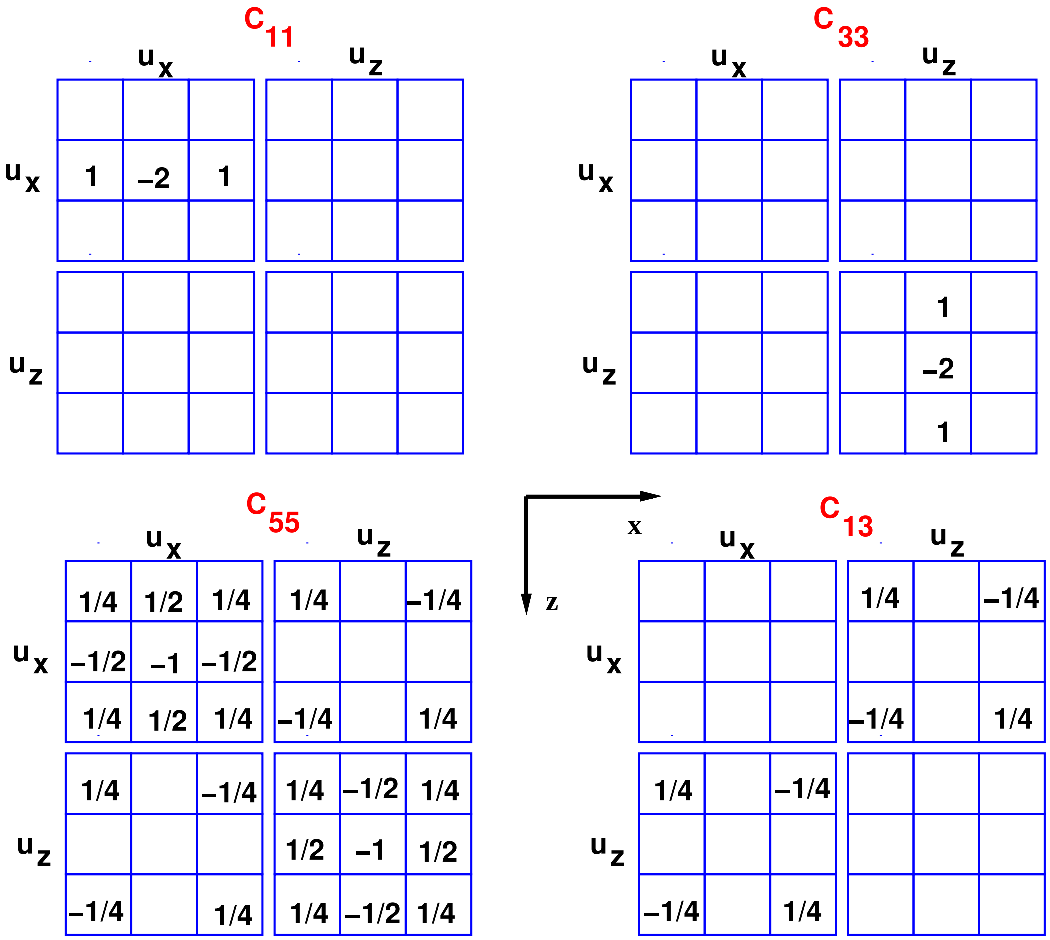

Figure 5: Differencing stars associated with the operator **A**. Each elastic constant contains four stars corresponding to the coupling between the two components (u_x and u_z) of the wavefield. Only the non-zero values are written. carlos2-star [NR]

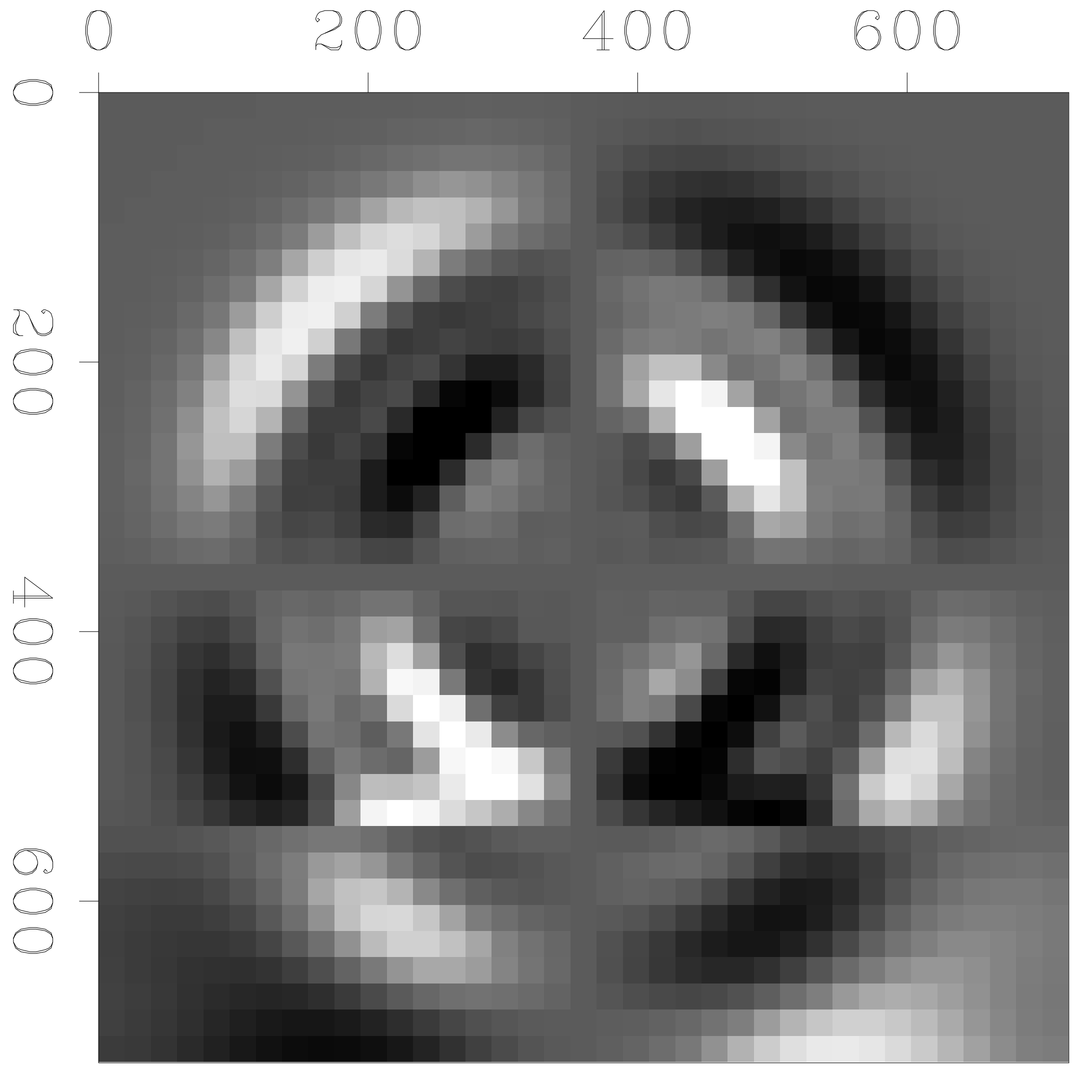

Figure 6: One frame of the horizontal displacement wavefield, for a vertical source using the eigenvalue-decomposition elastic modeling method. The upper 3/4 of the model is isotropic, while the bottom part is anisotropic. Because of the large computation time, the model size is 37 by 37 cells. Press the button to see a movie. carlos2-s2d1 [ER]

is the same used by Dablain (1986) to derive a fourth order in time, explicit, finite difference scheme. Contrary to the method presented here, Dablain's scheme used two time-step solutions ($\mathbf{u}(\mathbf{t}-\mathbf{\Delta t})$ and $\mathbf{u}(\mathbf{t})$) in order to find $\mathbf{u}(\mathbf{t}+\mathbf{\Delta t})$.

A recursive solution in the time domain can be obtained with the use of the following relations:

$$\frac{d^2\mathbf{u}(t)}{dt^2} = \mathbf{A}\mathbf{u}(t), \qquad \frac{d^3\mathbf{u}(t)}{dt^3} = \frac{d^2\dot{\mathbf{u}}(t)}{dt^2} = \mathbf{A}\dot{\mathbf{u}}(t), \qquad \frac{d^4\mathbf{u}(t)}{dt^4} = \mathbf{A}^2\mathbf{u}(t), \qquad \ldots,$$

in the Taylor expansion of $\mathbf{u}(t+dt)$ around $\mathbf{u}(t)$

$$\begin{aligned} \mathbf{u}(t+dt) &= \mathbf{u}(t) + \dot{\mathbf{u}}(t)dt + \frac{\mathbf{A}}{2}\mathbf{u}(t)dt^2 + \frac{\mathbf{A}}{6}\dot{\mathbf{u}}(t)dt^3 + \ldots \\ \dot{\mathbf{u}}(t+dt) &= \dot{\mathbf{u}}(t) + \mathbf{A}\mathbf{u}(t)dt + \frac{\mathbf{A}}{2}\dot{\mathbf{u}}(t)dt^2 + \frac{\mathbf{A}^2}{6}\mathbf{u}(t)dt^3 + \ldots \ . \end{aligned} \tag{7}$$

Combining these two equations, we obtain the time-propagation equation

$$\begin{pmatrix} \mathbf{u} \\ \dot{\mathbf{u}} \end{pmatrix}_{t+dt} \approx \mathbf{P}_+ \begin{pmatrix} \mathbf{u} \\ \dot{\mathbf{u}} \end{pmatrix}_t ,$$

where the forward time-propagation operator $\mathbf{P}_+$ has the following form:

$$\mathbf{P}_+ = \begin{bmatrix} \mathbf{I} + \frac{\mathbf{A}}{2}dt^2 & \mathbf{I}dt + \frac{\mathbf{A}}{6}dt^3 \\ \mathbf{A}\left(\mathbf{I}dt + \frac{\mathbf{A}}{6}dt^3\right) & \mathbf{I} + \frac{\mathbf{A}}{2}dt^2 \end{bmatrix} \tag{8}$$

for the case of a third-order approximation in time.

Figure **??** shows one frame of the horizontal displacement field, for the same source and media used to generate the synthetic data of Figure **??** (but with a finer grid spacing, and at a different time frame). This algorithm was implemented in the Connection Machine C2 with parellization in both spatial axes.

Stability and energy conservation associated with the truncation of the Taylor expansion in equation (8) are discussed in Appendix B.

CONCLUSIONS

Elastic modeling of a spatially-discrete system can be formulated as an eigenvalue decomposition problem. Using this formulation, the exact solution can be obtained for an arbitrarily complex model, without the need for time discretization. The unavoidable drawback of this formulation is its prohibitively high computing time, which is proportional to N^3, where N is the number of cells in the mesh. Building up a discrete physical model has some advantages over the usual numerical discretization of a continuous system. If the physical model is solved exactly, then stability is guaranteed since natural systems are always stable for impulsive sources. In addition,

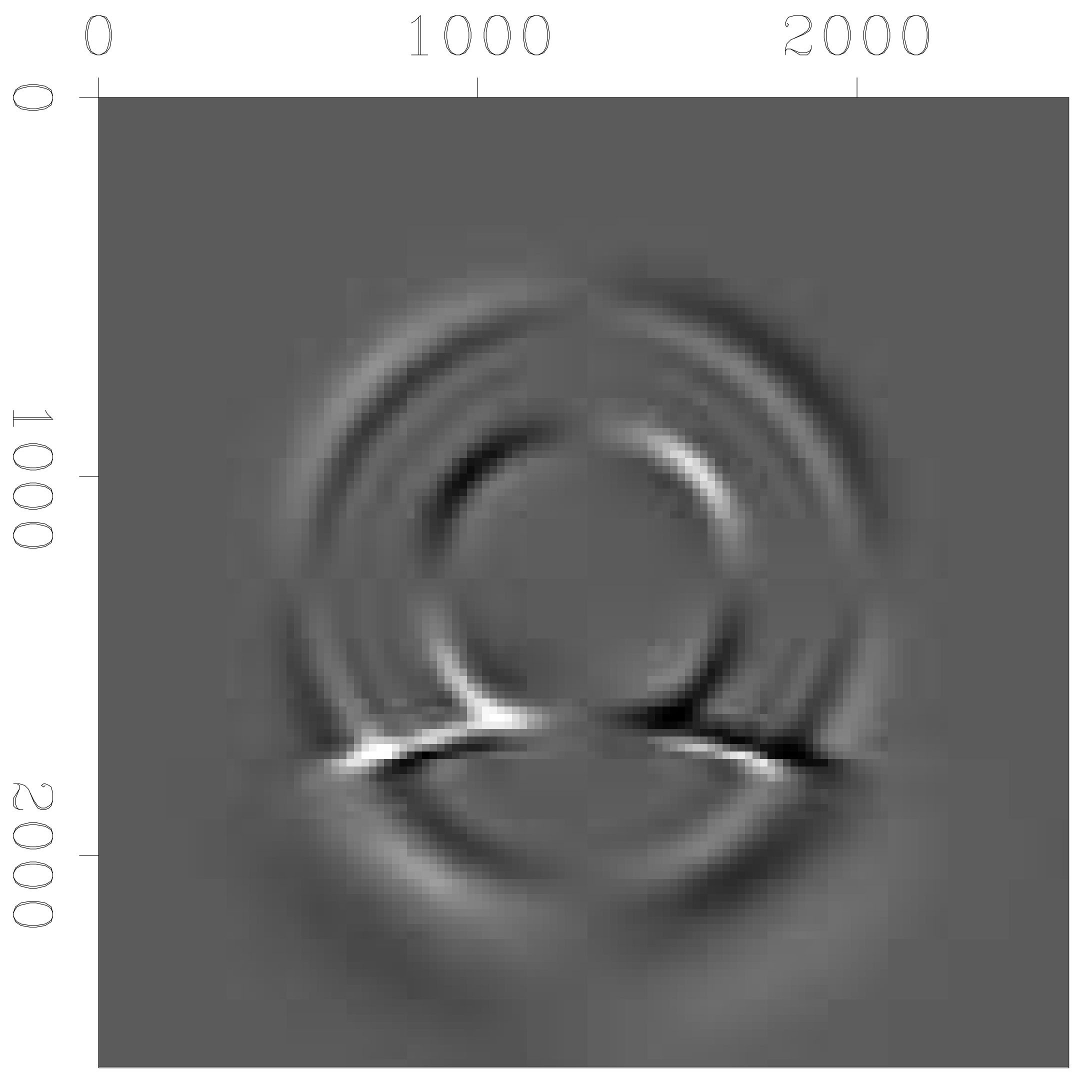

Figure 7: One frame of the horizontal displacement wavefield, for a vertical source using the recursive time-domain elastic modeling scheme. The upper 3/4 of the model is isotropic, while the bottom part is anisotropic. The model size is 129 by 129 cells and the algorithm is fourth order in time. Press the button to see a movie. carlos2-s2d2 [ER]

the resulting 2-D differencing star tends to cause less numerical anisotropy than the star obtained by straightforward discretization. An alternative solution in the time domain allows for an effective implementation of the modeling scheme in a massively parallel architecture machine.

REFERENCES

Auld, B.A., 1990, Acoustic fields and waves in solids, vol. I: Second edition, Kriegel Publishing Company.

Claerbout, J.F., 1985, Imaging the Earth's Interior: Blackwell Scientific Publications.

Dablain, M.A., 1986, The application of high-order differencing to the scalar wave equation: Geophysics, **51**, 54–66.

Etgen, J.T., 1989, Accurate wave equation modeling: SEP–**60**, 131–147.

Hale, D.T., 1990, 3-D depth migration via McClellan transformations: Presented at the 60th Ann. Internat. Mtg., Soc. Expl. Geophys., Expanded Abstracts, 1325–1328.

APPENDIX A

EQUATIONS OF MOTION FOR A 2-D TRANSVERSE ISOTROPIC DISCRETE SYSTEM

Figure **??**-a shows the 2-D elastic equivalent of the spring-mass model described in the paper. The medium is constituted by square cells with the mass concentrated in the center of the cell, and the elastic, massless part located at the boundaries. This elastic part is responsible for all the interaction between adjacent cells. As in the 1-D case, only adjacent cells can interact with each other. Therefore, the dynamics of cell $[i, j]$ in Figure **??**-a is controlled only by its own position, and the positions of its eight neighbor cells.

When a cell has a displacement component u, in the x or z direction, relative to its equilibrium position (Figure **??**-b), then one of its neighbor cells will be contracted by $u/2$ while the other neighbor will be expanded by $u/2$ if the system is homogeneous. For the case of heterogeneous systems, the contraction would be $\frac{c_2}{(c_1+c_2)}u$, where c_1 and c_2 are the stiffnesses (C_{11}) of the displaced and contracted cells, respectively.

It is sufficient to analyze the dynamics associated with the four basic displacements represented in Figures **??**-c to **??**-f since all the other cases can be easily derived from them. The following items refer to each of those figures in turn.

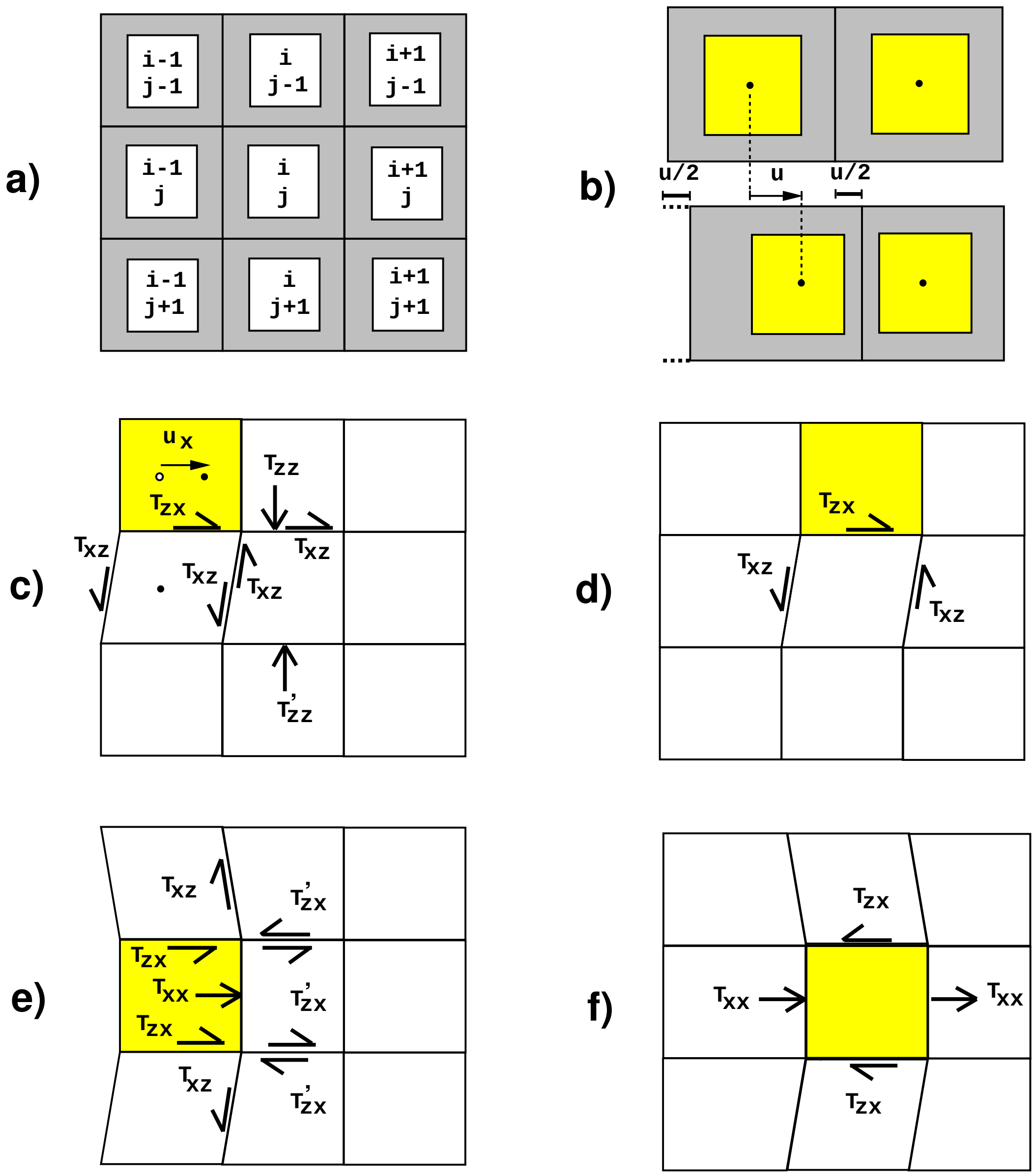

Figure 8: *(a)* A schematic model used to describe a 2-D elastic system. *(b)* Relations between the displacement of a cell and its neighbors. *(c)-(f)* The dynamics involved in the four basic displacements that interact with the central cell. The arrows represent some of the acting tractions and are located in the cell that is applying the traction. carlos2-blocks [NR]

- **case c**

  A displacement u_x in cell $[i-1, j-1]$ originates a shear traction T_{zx} between $[i-1, j-1]$ and $[i-1, j]$ (the traction applied by the first on the second is represented in the figure).

  $$T_{zx} = C_{55}\frac{u_x}{2L_x}$$

  where L_x is the x dimension of an undeformed cell. The rotational equilibrium requires that the total momentum applied to $[i-1, j]$ be zero. Therefore

  $$T_{xz} = \frac{T_{zx}}{2}.$$

  The same equilibrium condition in $[i, j]$, requires that the same shear traction T_{xz} be applied on it by $[i, j-1]$.

  The compression of $[i, j-1]$ by $u_x/2$ creates a compressional traction T_{zz} (associated with Young's moduli) between $[i, j-1]$ and $[i, j)$, while the asymmetrical compression of $[i, j]$ produces a compressional traction T'_{zz} between $[i, j]$ and $[i, j+1]$ given by the equations

  $$T_{zz} = C_{13}\frac{u_x}{2L_x} \qquad \text{and} \qquad T'_{zz} = -C_{13}\frac{u_x}{4L_x}.$$

  The total force applied in $[i, j]$ due to $[i-1, j-1]$'s displacement then has the following components:

  $$F_x = C_{55}\frac{u_x}{4}L_y \qquad \text{and} \qquad F_z = \{C_{13}\frac{u_x}{4} + C_{55}\frac{u_x}{4}\frac{L_z}{L_x}\}L_y.$$

- **case d**

  A displacement u_x in cell $[i, j-1]$ creates a shear traction T_{zx} between $[i, j-1]$ and $[i, j]$, whose magnitude is given by the equation

  $$T_{zx} = C_{55}\frac{u_x}{2L_x}.$$

  This traction will be responsible for the only net force applied in $[i, j]$, because the two shear tractions between $[i, j]$ and $[i-1, j]$, and between $[i, j]$ and $[i+1, j]$ compensate each other as well as the two compressional tractions (not represented in the figure) acting in the same interfaces.

  The total force applied in $[i, j]$ due to $[i, j-1]$'s displacement has only an x component, as follows:

  $$F_x = C_{55}\frac{u_x}{2}L_y.$$

- **case e**

A displacement u_x in cell $[i-1,j]$ creates a compressional traction T_{xx} between $[i-1,j]$ and $[i,j]$, and a shear traction T_{zx} between $[i-1,j]$ and $[i-1,j-1]$ whose magnitudes are given by the equations

$$T_{xx} = C_{11}\frac{u_x}{L_x} \qquad \text{and} \qquad T_{zx} = -C_{55}\frac{u_x}{2L_x}.$$

Applying the equilibrium conditions in $[i-1,j-1]$ and $[i,j-1]$, it follows that $T_{xz} = T'_{xz} = T_{zx}/2$. This traction is responsible for the only net force applied in $[i,j]$, because the two shear tractions between $[i,j]$ and $[i-1,j]$, and $[i,j]$ and $[i+1,j]$ compensate each other as well as the two compressional tractions (not represented in the figure) acting in the same interfaces.

The total force applied in $[i,j]$ caused by $[i-1,j]$'s displacement also has only an x component:

$$F_x = \{C_{11}u_x\frac{L_z}{L_x} - C_{55}\frac{u_x}{2}\}L_y.$$

- **case f**

  A displacement u_x in cell $[i,j]$ creates compressional tractions T_{xx} between $[i-1,j]$ and $[i,j]$, and between $[i,j]$ and $[i+1,j]$, and a shear traction T_{zx} between $[i,j-1]$ and $[i,j+1]$, whose magnitudes are given by the following equations:

  $$T_{xx} = -C_{11}\frac{u_x}{L_x} \qquad \text{and} \qquad T_{zx} = -C_{55}\frac{u_x}{2L_x}.$$

  The total force applied in $[i,j]$ caused by $[i,j]$'s displacement also has only an x component, as follows:

  $$F_x = -\{2C_{11}u_x\frac{L_z}{L_x} + C_{55}\frac{u_x}{2}\}L_y$$

For the more general heterogeneous case, some definitions are required to simplify the equations of motion:

- For the stiffness constants, the cells are identified by a number: $[i-1,j-1] \equiv 1$, $[i,j-1] \equiv 2$, ..., $[i,j] \equiv 5$, ..., $[i+1,j+1] \equiv 9$.
- Two equivalent elastic tensors are defined by:

$$W^{k,l}_{mn} = \frac{C^k_{mn}}{C^k_{mn} + C^l_{mn}} \qquad \text{and} \qquad \bar{C}^{k,l}_{mn} = 2\frac{C^k_{mn}C^l_{mn}}{C^k_{mn} + C^l_{mn}}$$

Taking the contributions from the x and z displacements of all nine cells into account leads to the following equations of motion for cell $[i,j]$:

$$\rho^{i,j}L_xL_z\frac{d^2u^{i,j}_x(t)}{dt^2} = C^1_{55}\frac{u^{i-1,j-1}_x}{4} + C^3_{55}\frac{u^{i+1,j-1}_x}{4} + C^7_{55}\frac{u^{i-1,j+1}_x}{4} + C^9_{55}\frac{u^{i+1,j+1}_x}{4}$$

$$
\begin{aligned}
&+C_{55}^{2}\frac{u_x^{i,j-1}}{2}+C_{55}^{8}\frac{u_x^{i,j+1}}{2}+\{\bar{C}_{11}^{4,5}\frac{L_z}{L_x}\ -\frac{C_{55}^{4}}{2}\}u_x^{i-1,j}\\
&+\{\bar{C}_{11}^{5,6}\frac{L_z}{L_x}\ -\frac{C_{55}^{6}}{2}\}u_x^{i+1,j}-\{(\bar{C}_{11}^{4,5}+\bar{C}_{11}^{5,6})\frac{L_z}{L_x}\ +C_{55}^{5}\}u_x^{i,j}\\
&+\{W_{11}^{1,2}C_{13}^{2}-\frac{W_{11}^{4,5}C_{13}^{5}}{2}+\frac{C_{55}^{1}}{4}\frac{L_z}{L_x}\ \}u_z^{i-1,j-1}\\
&-\{W_{11}^{3,2}C_{13}^{2}-\frac{W_{11}^{6,5}C_{13}^{5}}{2}+\frac{C_{55}^{3}}{4}\frac{L_z}{L_x}\ \}u_z^{i+1,j-1}\\
&-\{W_{11}^{7,8}C_{13}^{8}-\frac{W_{11}^{4,5}C_{13}^{5}}{2}+\frac{C_{55}^{7}}{4}\frac{L_z}{L_x}\ \}u_z^{i-1,j+1}\\
&+\{W_{11}^{9,8}C_{13}^{8}-\frac{W_{11}^{6,5}C_{13}^{5}}{2}+\frac{C_{55}^{9}}{4}\frac{L_z}{L_x}\ \}u_z^{i+1,j+1},
\end{aligned}
$$

$$
\begin{aligned}
\rho^{i,j} L_x L_z \frac{d^2 u_z^{i,j}(t)}{dt^2} \quad = \quad & C_{55}^1 \frac{u_z^{i-1,j-1}}{4} + C_{55}^7 \frac{u_z^{i-1,j+1}}{4} + C_{55}^3 \frac{u_z^{i+1,j-1}}{4} + C_{55}^9 \frac{u_z^{i+1,j+1}}{4} \\
& + C_{55}^4 \frac{u_z^{i-1,j}}{2} + C_{55}^6 \frac{u_z^{i+1,j}}{2} + \{\bar{C}_{33}^{2,5} \frac{L_x}{L_z} - \frac{C_{55}^2}{2}\} u_z^{i,j-1} \\
& + \{\bar{C}_{33}^{5,8} \frac{L_x}{L_z} - \frac{C_{55}^8}{2}\} u_z^{i,j+1} - \{(\bar{C}_{33}^{2,5} + \bar{C}_{33}^{5,8}) \frac{L_x}{L_z} + C_{55}^5\} u_z^{i,j} \\
& + \{W_{33}^{1,4} C_{13}^4 - \frac{W_{33}^{2,5} C_{13}^5}{2} + \frac{C_{55}^1}{4} \frac{L_x}{L_z}\} u_x^{i-1,j-1} \\
& - \{W_{33}^{7,4} C_{13}^4 - \frac{W_{33}^{8,5} C_{13}^5}{2} + \frac{C_{55}^7}{4} \frac{L_x}{L_z}\} u_x^{i-1,j+1} \\
& - \{W_{33}^{3,6} C_{13}^6 - \frac{W_{33}^{2,5} C_{13}^5}{2} + \frac{C_{55}^3}{4} \frac{L_x}{L_z}\} u_x^{i+1,j-1} \\
& + \{W_{33}^{9,6} C_{13}^6 - \frac{W_{33}^{8,5} C_{13}^5}{2} + \frac{C_{55}^9}{4} \frac{L_x}{L_z}\} u_x^{i+1,j+1}.
\end{aligned}
$$

APPENDIX B

STABILITY AND ENERGY CONSERVATION

Stability requires the conservation of energy during the time propagation process. For the elastic system considered here, the conservation of energy is represented by (Auld, 1990):

$$
\begin{pmatrix} \mathbf{u} \\ \dot{\mathbf{u}} \end{pmatrix}^T \begin{bmatrix} -\mathbf{A} & \mathbf{0} \\ \mathbf{0} & \mathbf{I} \end{bmatrix} \begin{pmatrix} \mathbf{u} \\ \dot{\mathbf{u}} \end{pmatrix} = \begin{pmatrix} \mathbf{u} \\ \dot{\mathbf{u}} \end{pmatrix}^T \mathbf{P}_+^{\mathbf{T}} \begin{bmatrix} -\mathbf{A} & \mathbf{0} \\ \mathbf{0} & \mathbf{I} \end{bmatrix} \mathbf{P}_+ \begin{pmatrix} \mathbf{u} \\ \dot{\mathbf{u}} \end{pmatrix}. \tag{9}
$$

Using the approximation for $\mathbf{P}_+$ given by equation (8) the righthand side becomes

$$
\begin{pmatrix} \mathbf{u} \\ \dot{\mathbf{u}} \end{pmatrix}^T \begin{bmatrix} -\mathbf{A} & \mathbf{0} \\ \mathbf{0} & \mathbf{I} \end{bmatrix} \begin{bmatrix} (\mathbf{I} + \frac{\mathbf{A}}{2} dt^2)^2 & -\mathbf{A}(\mathbf{I}dt + \frac{\mathbf{A}}{6} dt^3)^2 \\ (\mathbf{I} + \frac{\mathbf{A}}{2} dt^2)^2 & -\mathbf{A}(\mathbf{I}dt + \frac{\mathbf{A}}{6} dt^3)^2 \end{bmatrix} \begin{pmatrix} \mathbf{u} \\ \dot{\mathbf{u}} \end{pmatrix},
$$

and equation (9) assumes the form

$$
\begin{pmatrix} \mathbf{u} \\ \dot{\mathbf{u}} \end{pmatrix}^T \begin{bmatrix} -\mathbf{A} & \mathbf{0} \\ \mathbf{0} & \mathbf{I} \end{bmatrix} \begin{pmatrix} \mathbf{u} \\ \dot{\mathbf{u}} \end{pmatrix} = \begin{pmatrix} \mathbf{u} \\ \dot{\mathbf{u}} \end{pmatrix}^T \begin{bmatrix} -\mathbf{A} & \mathbf{0} \\ \mathbf{0} & \mathbf{I} \end{bmatrix} \mathbf{P}_- \; \mathbf{P}_+ \begin{pmatrix} \mathbf{u} \\ \dot{\mathbf{u}} \end{pmatrix}. \tag{10}
$$

Equation (10) shows that the energy conservation, and thus the stability of the extrapolation process, is controlled by how well the consecutive application of the forward and backward propagation operators can reproduce the original wavefield.